Environmental Chemistry and Ecotoxicology 1 (2019) 49–60

Contents lists available at ScienceDirect

Environmental Chemistry and Ecotoxicology

journal homepage: www.keaipublishing.com/en/journals/environmental-chemistry-and-ecotoxicology/

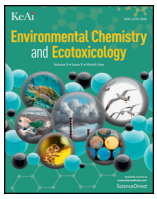

Characterization and bioaccessibility assessment of elements in urban aerosols by extraction with simulated lung fluids

Hanne Weggeberg [a,*], Tonje Fagertun Benden [b], Syverin Lierhagen [a], Eiliv Steinnes [a], Trond Peder Flaten [a]

[a] Department of Chemistry, Norwegian University of Science and Technology (NTNU), NO-7491 Trondheim, Norway
[b] Norwegian Veterinary Institute, Pb 5695 Torgarden, NO-7485 Trondheim, Norway

ARTICLE INFO

Article history:
Received 27 June 2019
Received in revised form 14 October 2019
Accepted 16 October 2019
Available online 15 November 2019

Keywords:
Airborne particulate matter
Trace elements
Seasonal differences
Metal bioaccessibility
Simulated lung fluids

ABSTRACT

Airborne particulate matter (PM) size fractions $PM_{2.5–10}$ (coarse), $PM_{0.1–2.5}$ (fine) and $PM_{0.1}$ (ultrafine) were collected from a site affected by high traffic and a city background site within the city of Trondheim, Norway during spring and winter periods. Concentrations of a range of elements in the different size fractions were determined using high-resolution inductively-coupled plasma mass spectrometry (HR-ICP-MS), and bioaccessibility of the elements was assessed by extraction in Gamble's solution (GMB) and artificial lysosomal fluid (ALF).

Samples from the trafficked site generally showed higher PM and HNO_3 soluble element concentrations than those from the background site. Concentrations of the typical crustal elements Sc, Al, and W were higher in PM collected in spring (March–April) than in winter (December–January), whereas concentrations of most of the assumed primarily vehicle-derived elements, namely As, Cd, and Cu were highest in winter.

Principal component analysis (PCA) indicated re-suspension of soil-derived elements and motor vehicle emissions as the major sources of most elements. Enrichment factor values were particularly high for Sb, indicating this element as a valuable marker for vehicular road traffic emissions.

The solubility was highly variable among the elements, but overall considerably higher in ALF compared to GMB. Interestingly, most elements had lower solubility in the ultrafine than in the fine size fraction. In conclusion, the levels of PM and its elemental components are generally quite low in Trondheim, but certain elements including Tl, As, W, Sb, and Cu may be readily soluble within the lung and thereby bioaccessible and of potential toxicological concern.

1. Introduction

Air pollution, and particularly airborne particulate matter (PM) components, is a major environmental health issue especially in urban areas and is responsible for a considerable proportion of deaths and disease worldwide [1]. Exposure to PM is associated mainly with respiratory and cardiovascular mortality and diseases [2–4].

PM originates from various sources, both natural, such as suspended soil particles, and anthropogenic, including motor vehicles, industrial activities and domestic stove heating. Primary particles are emitted directly into the atmosphere, whereas secondary particles are formed through chemical reactions. These complexities in origin and physicochemical processes result in large spatial and temporal variations in atmospheric concentration, size distribution, and chemical composition of PM. PM is generally classified into coarse, fine, and ultrafine particles according to aerodynamic diameter, based on the depth in the respiratory system to which the particles are likely to penetrate and deposit. The coarse fraction, often denoted $PM_{2.5–10}$, comprises all particles with aerodynamic diameter between 2.5 and 10 μm, which are likely to reach and deposit in the bronchi. Fine PM is particles with aerodynamic diameter between 0.1 and 2.5 μm, which primarily deposit in the terminal bronchi and alveoli, whereas the ultrafine fraction consists of particles < 0.1 μm, which are able to penetrate deeper into the lungs, and may also cross the air-blood barrier [5]. Thus, particle size is one of the main determinants for deposition in the respiratory tract, and thus for PM toxicity. Ultrafine particles are of special concern due to their ability to enter the blood stream directly and have potential adverse effects on cardiovascular conditions. Moreover their high particle number by mass and surface to volume ratio provide numerous potential binding sites for easily soluble chemical components.

Numerous studies have attempted to determine which components of PM are responsible for the observed adverse health effects. Some elemental components have been considered to be likely causative agents in PM toxicity, primarily due to their ability to directly or indirectly produce reactive oxygen species (ROS) in biological tissues [6,7].

While the majority of studies investigating elemental composition of PM measured the total atmospheric concentrations, information on the solubility of elements is important since this fraction is likely to be the most bioaccessible, *i.e.* available for uptake in cells, and thereby potentially

* Corresponding author at: Rambøll i Norge AS, Pb 9420, NO-7493 Trondheim, Norway.
E-mail address: hanne.weggeberg@ramboll.no. (H. Weggeberg).

Production and hosting by Elsevier on behalf of KeAi

http://dx.doi.org/10.1016/j.enceco.2019.10.001

exerting toxicity [8–10]. Simulated lung fluids (SLFs) offer valuable tools in assessment of elemental PM component bioaccessiblity. Investigating element solubility in SLFs is preferable to simpler chemical leaching with agents such as water or weak acids since the former mimic the actual biological fluids found in the lungs in a relatively simple and inexpensive way. Gamble's solution (GMB) has a composition that simulates the interstitial fluid within the deep lung under normal health conditions, whereas artificial lysosomal fluid (ALF) represents the acidic intracellular conditions in lung cells following phagocytosis under stressed conditions [11–13]. SLFs have been used extensively to investigate the bioaccessibility of industrially produced compounds [11,14]. In recent years, a number of studies have utilized SLFs to assess the bioaccessibility of PM samples. Colombo et al. [15] and Zereini et al. [16] used GMB and ALF to investigate the mobility of platinum group elements in PM. Wiseman and Zereini [17] assessed the solubility of several metals and metalloids in different size fractions of urban PM. Although extraction in SLFs is a well established methodology for studying bioaccessibility of PM constituents, more knowledge is needed regarding the total concentrations and solubility of a wider range of PM elemental components at different sites and seasons. Relatively few studies have included the ultrafine size fraction in metal content studies of urban PM, and there is a particular scarcity of studies that compare the coarse, fine, and ultrafine fractions.

The aims of the present study were to investigate the levels of a range of elemental components of PM within the coarse, fine and ultrafine size fractions at two different urban sites within the city of Trondheim, Norway, and to assess the origin of these elements using enrichment factors (EFs) and principal component analysis (PCA), and their bioaccessibility using GMB and ALF.

2. Methods

2.1. Description of test sites

Trondheim is the fourth most populated urban area in Norway, with a population of 177,617 in January 2016 [18]. $PM_{2.5–10}$ (coarse), $PM_{0.1–2.5}$ (fine), and $PM_{0.1}$ (ultrafine) aerosol fractions were collected from two municipal air measurement stations within Trondheim, representing two different exposure scenarios: Elgeseter station is located at street level nearby a main road, whereas Torget is the urban background station, placed 15 m above ground level on the roof of Torget shopping mall in the city center (Fig. 1) [19]. Elgeseter street is the most heavily trafficked road in Trondheim, with a daily average of 20,500 passing motor vehicles. Torget represents city background levels where the primary background PM sources involve emissions from bus traffic and domestic heating. Atmospheric $PM_{10,}$ $PM_{2.5}$ and NO_2 concentrations are measured routinely at these two stations according to the European Union Directive 2008/50/EC [20]. At Elgeseter all measurement and collection equipment is placed inside a temperature-regulated stall, whereas at Torget the sampling equipment is housed in a separate temperature-controlled locker (Industriell Måleteknikk, Norway). The Norwegian Public Roads Administration and Trondheim Municipality operate Elgeseter and Torget stations, respectively.

2.2. Collection and preparation of PM samples

PM samples were collected during five consecutive periods in spring (March–April 2014) and in winter (December 2014 to January 2015) simultaneously at Elgeseter and Torget stations, yielding a total of 60 samples; five samples from each site during each season within each of the three size fractions ($PM_{2.5–10}$, $PM_{0.1–2.5}$, and $PM_{0.1}$). Sample collection and analysis which included all three size fractions had to be limited to shorter time periods to limit costs. $PM_{0.1}$ samples were collected and analyzed as part of the same project for an extended time period; results from this work are presented in a separate article [21]. In urban areas in Norway, PM concentrations are typically elevated in periods during winter when emissions from sources such as wood burning and road salt and sand are higher, and in spring when the roads dry up and exposed silt is resuspended. The duration of sampling for individual samples varied from 144 to 216 h to ensure sufficient particle mass on the filters for analysis,

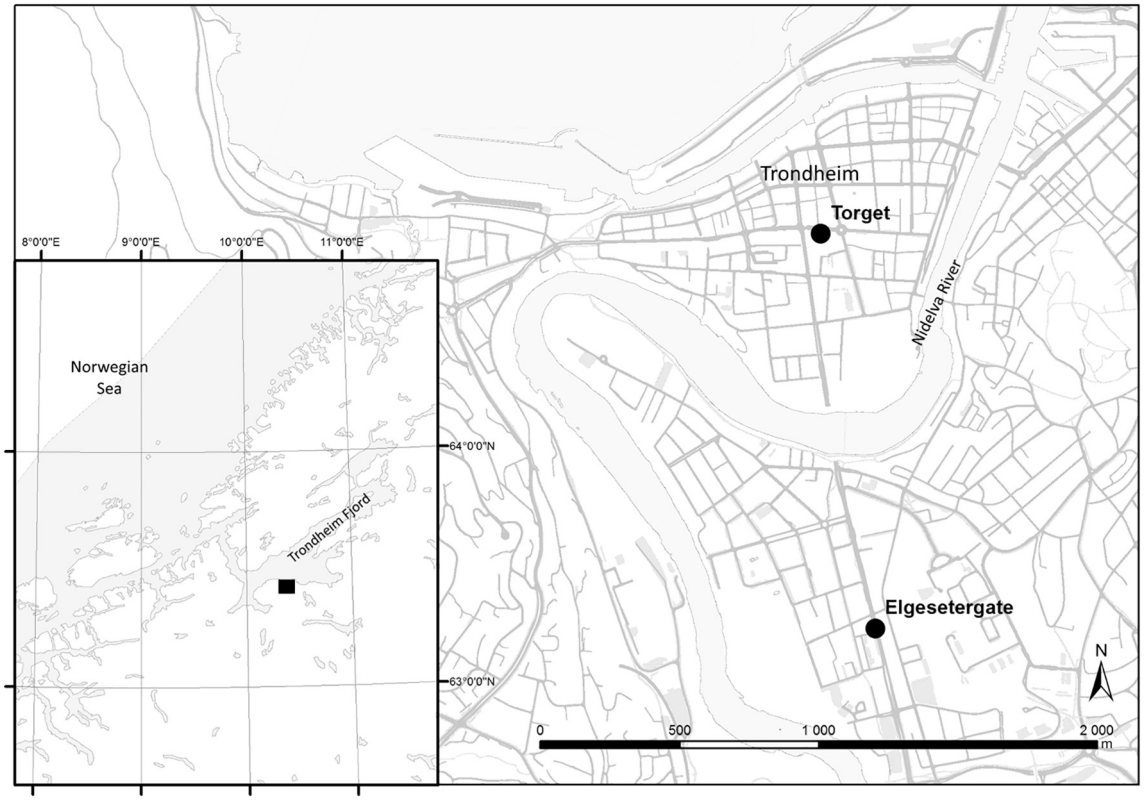

Fig. 1. Map showing the two test sites for PM collection: Elgeseter and Torget.

depending on expected ambient PM concentrations based on season, temperature, precipitation and road dust reduction measures taken.

PM was collected with Moudi cascade impactors model 100-S4 Special from MSP/Copley Scientific, equipped with pressure gauges and flow meters model DFM2000, both from Copley Scientific, and low capacity pumps model LCP5 from Copley Scientific or membrane pumps. The flow rate used was 30 ± 1 L/min. The impactors were placed at each measurement station, and connected to TSP inlets from Digitel with 1 m long tubes, resulting in the inlets being about 4 and 17 m above the ground at Elgeseter and Torget, respectively. The impactors had cut-points of 18, 10, 2.5 and 0.1 μm, thereby separating the PM into five stages: >18, 10–18, 2.5–10 (coarse), 0.1–2.5 (fine), and <0.1 μm (ultrafine fraction), with one filter at each impaction stage. Element contents and solubility in SLFs were determined in samples from the last three stages, which correspond to $PM_{2.5–10}$, $PM_{0.1–2.5}$, and $PM_{0.1}$, respectively. Zefluor PTFE filters from VWR with pore size of 2.0 μm and diameter 47 mm were used as impaction substrates.

Gravimetric determination of particle mass was performed according to European Standard EN 12341:2014 [22]. The filters were weighed prior to and after particle loading. Unloaded and loaded filters were conditioned for 48 h prior to weighing, and then for another 24 h before weighed a second time; the maximum acceptable difference between these two masses was set to 0.5 mg. The methodology for the gravimetry is explained in further detail in the Supplementary Material. Particle mass was calculated by subtracting the average unloaded from the loaded filter mass. After weighing, the filters were stored in the petri dishes in an ISO 6 cleanroom until assembly in the impactors for the unloaded (no >28 days) or SLF extraction for the loaded filters.

2.3. Simulated lung fluid (SLF) preparation and extraction

The SLFs were prepared in Teflon bottles according to Herting et al. [11], with ALF among other constituents containing citric acid. pH was adjusted using NaOH (50%) and HCl (25%), to 7.4 and 4.5 for GMB and ALF, respectively. Filters loaded with PM were then cut in half with steel scissors or a scalpel, and placed inside polyethylene vessels (15 mL) using plastic tweezers. 5 mL test media was added to the filter pieces that contained on average about 0.5 mg particles. The vessels were placed in an incubator and subjected to bilinear shaking at 125 cycles per min. at 37 ± 0.5 °C for 24 h. At the end of the extraction period pH was measured in selected samples to check that pH in the test media had not changed significantly. After incubation the filters were removed using plastic tweezers and placed in 15 mL polyethylene vessels, after which the solutions were centrifuged for 10 min. at 710 relative centrifugal force (rcf).

2.4. Determination of elements by ICP-MS

The supernatant was decanted into a 15 mL polyethylene vessel, acidified with concentrated HNO_3 and diluted with deionized water to 0.6 M HNO_3 for element analysis. 2 mL 50% v/v HNO_3 was added to the precipitate, before transferring it to a 18 mL Teflon UltraClave vessel, and the precipitate was dissolved together with the filter using an UltraClave ultrawave-assisted autoclave (Milestone) in which the temperature and pressure rose gradually to 245 °C and 160 bar. After dissolution the samples were diluted with deionized water to a final HNO_3 concentration of 0.6 M, and then transferred to cleaned 15 mL polyethylene tubes. Acidified supernatant and precipitate samples were stored at room temperature until element analysis.

Concentrations of elements in supernatant and precipitate samples were determined using high-resolution inductively-coupled plasma mass spectrometry (HR-ICP-MS, Thermo Finnigan Element 2 from Thermo Fisher Scientific). Thus, concentrations in supernatant samples represented the element fraction that was soluble in SLFs (Gamble's solution and ALF), whereas the sum of the concentrations in supernatant and precipitate samples represented the HNO_3 soluble or "pseudototal" element fraction. An SC-FAST flow injection system for SC-4 from ESI was used. Two multi-element solutions (PS-ClBrI and PS-70, both from ESI) were used: One as a calibration solution used prior to sample introduction and then after every tenth sample, and one as a quality control sample to test for accuracy. Three different dilutions of the calibration solution were prepared and used. An internal standard (rhenium, 1 μg/L) was automatically added to each sample. To avoid interferences three different mass resolutions were applied: low (400), medium (4000), and high (10000). The elements determined were: Ag, Al, As, Au, B, Ba, Be, Bi, Cd, Ce, Co, Cr, Cs, Cu, Dy, Er, Fe, Ga, Hf, Hg, Ho, Ir, La, Li, Lu, Mg, Mn, Mo, Nb, Nd, Ni, Pb, Pr, Pt, Rb, Sb, Sc, Si, Sm, Sn, Sr, Ta, Tb, Th, Ti, Tl, Tm, U, V, W, Y, Yb, Zn, and Zr. Limits of detection (LODs) were calculated as three times the standard deviation of element concentrations in the blank sample replicates. The instrumental limits of quantitation (LOQs) for each element correspond to the concentrations which yield relative standard deviations (RSDs) of 25%.

2.5. Quality control

Measures were taken to minimize contamination during all stages of the experimental process (see Supplementary Material).

The Moudi cascade impactors stage bodies were cleaned regularly in deionized water and methanol to ensure that the pressure did not drop significantly, and flow meters were calibrated yearly, all in accordance with recommendations from the suppliers.

Field blank samples consisted of filters that were conditioned, weighed, stored, transported to the test sites and assembled in the impactors in the field but without adding flow, and extracted by the same methods as the PM sample filters. Urban Particulate Matter (UPM) 1648a from NIST, Urban Aerosols (UA) No. 28 from NIES, and Polish Virginia Tobacco Leaves (PVTL) 6 from ICHTJ were used as standard reference materials (SRMs). SRM samples (1.5–50 mg) were extracted following the same procedure as the particulate and blank samples. ICP-MS precision was estimated by analyzing the same sample three times and calculating relative standard deviations (RSDs), whereas reproducibility of filter element concentrations was checked by cutting filters in two from the different test sites and size fractions and treating the two halves identically (five filters for each size fraction and for each type of SLF). Elements present at low concentrations with significant proportions below detection limits, with high RSDs, poor reproducibility, and/or with low SRM recovery were excluded from further analysis.

The analytical precision was satisfactory for most of the elements studied, with mean relative standard deviations (RSDs) below 10% (results not shown). Pt was the most notable exception, with RSDs generally above 35%, and it was therefore excluded from further discussion. Cd, Tl, and As had mean RSDs between 10 and 35%. Mean RSDs were generally higher in SLF-soluble than in insoluble fraction samples. Reproducibility was generally satisfactory, with ratios between replicate samples typically between 0.7 and 1.3, and Pearson correlation coefficients above 0.6 for the elements studied (results not shown). Correlation coefficients were generally lower for dissolved than for precipitate fraction samples. SRM results indicated overall somewhat low and variable recoveries for most elements for the extraction methods used (Table 6): UPM 1648a showed overall low recoveries, typically between 40 and 60%, whereas UA No. 28 gave recoveries of about 10 to 20 percentage points higher for the same elements.

2.6. Statistical analysis

Enrichment factors (EFs) were used as indicators of sources of elemental constituents of the PM samples [23], and were estimated according to the following formula:

$$EF_X = \left([X]_{sample}/[Al]_{sample}\right)/\left([X]_{crust}/[Al]_{crust}\right)$$

where X is the element under consideration using Al as the reference element, and the average crustal concentrations used accordingly to Mason and Moore [24]. EF values may provide information on the proportion of airborne elements originating from anthropogenic sources. Values larger

than 1 imply some anthropogenic contribution, and EF > 10 strongly indicates that the element in question is predominantly of anthropogenic origin [25].

Differences in element HNO_3 soluble concentrations between test sites and solubility in GMB and ALF were investigated using the nonparametric Mann-Whitney *U* test. Statistical significance is denoted at the 0.05 p-value throughout. Correlations between elemental HNO_3 soluble contents were examined using principal component analysis (PCA) to investigate and identify possible sources of the PM. PCA was performed on scaled and centered concentration data. The validity of the PCA models was assessed with Kaiser-Meyer-Olkin Measure of Sampling Adequacy (KMO) and Bartlett's Test of Sphericity (Bartlett's test), as well as with split-sample validation. Correlation biplots were constructed with coefficient 1, meaning that the length of the variable vectors correspond to the standard deviations. Element concentration values below the LODs were imputed by a method of constrained maximization of the Shapiro-Wilk *W* statistic [26]. Element variables for which the Pearson correlation coefficients for replicates after dissolution in HNO_3 were below 0.7 were excluded from simulated lung fluid solubility analysis. Statistical treatment was conducted with SPSS 22.0, XLStat 2015.2.02, and R 3.2.0.

3. Results and discussion

3.1. PM levels

Total PM concentrations within the coarse ($PM_{2.5–10}$), fine ($PM_{0.1–2.5}$), and ultrafine ($PM_{0.1}$) size fraction at the two measurement stations, collected during spring and winter season, were generally low (Table 1). The concentrations varied substantially, and the data were right-skewed and lognormally distributed, as shown by tests of normality and probability plots (not shown). As expected, except for $PM_{2.5–10}$ in winter, levels were overall higher at the Elgeseter roadside station compared to the Torget urban background station, especially in the coarse fraction, but none of these differences were statistically significant at the 0.05 level. At Elgeseter, median $PM_{2.5–10}$ concentrations were 2.3 times higher in spring than in winter samples, statistically significant at the 0.05 level, whereas concentrations in spring and winter were similar at Torget. On the other hand, $PM_{0.1–2.5}$ and $PM_{0.1}$ concentrations were highest in winter, both at Elgeseter and Torget. This is consistent with municipal routine air quality measurements, which show that $PM_{2.5}$ concentrations generally are highest during the winter season, whereas the $PM_{2.5–10}$ fraction levels usually peak at short periods during spring (March–April) [19].

Of the three size fractions investigated, coarse mass concentrations in air were highest, followed by fine and finally ultrafine mass concentrations. Several other studies measuring mass concentrations in different PM size fractions in urban areas report considerably higher PM levels and often the highest mass concentrations in the fine fraction; for instance, Gugamsetty et al. [27] reported average PM_{10}, $PM_{2.5}$ and $PM_{0.1}$ concentrations of 39, 22, and 1.4 μg/m^3, whereas Lin et al. [28] found mean air concentrations of 51, 140, and 31 μg/m^3 in the same fractions near a heavily trafficked road. Thus, particle size distributions show considerable spatial variations in urban areas, depending on type of and distance to particle emission sources. However, relatively few studies have included $PM_{0.1}$, and especially size fraction distributions between coarse, fine and ultrafine fractions.

All recorded values were well below the limit values set by the EU Directive 2008/50/EC [20] of 40 μg/m^3 for a calendar year for PM_{10} (which corresponds to the sum of the $PM_{2.5–10}$, $PM_{0.1–2.5}$ and $PM_{0.1}$ size fractions) and correspondingly 25 μg/m^3 for $PM_{2.5}$ (the sum of $PM_{0.1–2.5}$ and $PM_{0.1}$). However, the sampling periods use in the present study (144–216 h) do not allow for direct comparison to these limit values; concentrations may have been elevated during short time periods. Indeed, municipal routine measurements showed exceedances of the PM_{10} daily limit value of 50 μg/m^3 on certain days both at Elgeseter and Torget during the collection period [19]. No 24-hour value exists for $PM_{2.5}$, and limit values for $PM_{0.1}$ have not been established. Environmental health studies have, however, found associations between long-term exposure to chronic $PM_{2.5}$ levels below EU regulatory limit values and mortality [1,29].

3.2. Uncertainties

The PM_{10} and $PM_{2.5}$ atmospheric concentrations measured in this study were typically 40–60% of the routine measurements conducted by Trondheim Municipality and the Norwegian Public Roads Administration during the same time periods (results not shown), indicating that the sampling efficiency of the cascade impactors used was low. Possible bounce of particles and resulting contamination of lower size impaction stages of larger particles was examined in representative samples using scanning electron microscopy (SEM). The SEM analysis showed that the collected particle samples seemed for the most part to contain particles within the correct size range, with only a very small number of larger contaminating particles. This examination is presented in more detail in the Supplementary Material. Also, the HNO_3 soluble fractions measured in this study might underestimate the total element concentrations in the samples. Recoveries for the HNO_3 soluble fractions for the SRM Urban Aerosols No. 28 (NIES), and for both HNO_3 and HF soluble fractions for Soil GBW 07408, are summarized in Supplementary Table 4.

For some of the elements included in the SLF analysis considerable proportions of the concentration values, especially for supernatant (SLF soluble) fraction samples, were below the respective LOQ values (Tables 7–9). Results for which supernatant and/or precipitate (HNO_3 soluble) concentrations were below the corresponding LOQ were not included in the solubility calculations. SLF solubility values for elements in SRM (NIST 1648a), compared to certified values, were overall considerably lower compared to those obtained for the studied PM samples for several of the elements studied (Table 10). For SRM samples, the highest solubility was observed for As (GMB: mean 19 ± 13%; ALF: 43 ± 29%) and the lowest for Cr, Ce, Al, and Pb. As found for the PM samples collected in the study, element solubility was substantially higher in ALF than in GMB.

3.3. PM elemental constituents

Levels of the element constituents within all three size fractions of PM were variable, but overall low; in the pg/m^3 range for most elements

Table 1
Total airborne particulate matter (PM) contents (in μg/m^3) in road traffic (Elgeseter) and city background (Torget) samples, in coarse ($PM_{2.5–10}$), fine ($PM_{0.1–2.5}$), and ultrafine ($PM_{0.1}$) size fractions. N = 5 from each site and season for each size fraction.

	Spring									Winter									Spring/winter median ratio	
	Elgeseter				Torget					Elgeseter				Torget					Elgeseter	Torget
	Median	Mean	SD	Range	Median	Mean	SD	Range	Ratio	Median	Mean	SD	Range	Median	Mean	SD	Range	Ratio*		
$PM_{2.5-10}$	3.9	4.9	2.9	2.2–9.7	2.2	2.0	1.1	0.39–3.2	2.4	1.7	1.8	0.6	1.1–2.6	1.5	2.1	1.5	0.70–3.8	0.9	**2.3**	1.5
$PM_{0.1–2.5}$	1.1	1.3	0.7	0.68–2.6	1.4	1.2	0.7	0.02–1.6	1.1	2.3	2.3	0.6	1.3–2.8	2.0	1.9	0.4	1.3–2.4	1.2	0.5	**0.7**
$PM_{0.1}$	1.2	1.5	0.8	0.74–2.9	0.90	0.92	0.2	0.77–1.2	1.6	1.3	1.5	0.7	0.67–2.6	1.0	1.2	0.3	0.84–1.6	1.3	0.9	0.9

* Ratios in bold signify statistically significant differences between the spring and winter values at the 0.05 level, calculated using the Mann-Whitney *U* test.

Table 2
Total element contents (in μg/g, unless otherwise stated) in road traffic (Elgeseter) and city background (Torget) $PM_{2.5–10}$ samples, collected in spring and winter (N = 5 from each site and for each season). p-Values in bold signify statistical significance at the 0.05 level, whereas p-values in bold and italic signify statistical significance at the 0.01 level.

	Spring				Winter				Spring/winter ratio			
	Elgeseter		Torget		Elgeseter		Torget		Elgeseter	Torget		
	Median	IQR[a]	Median	IQR	Median	IQR	Median	IQR			LOD[b]	% < LOD
Al (mg/g)	38	32–39	26	26–32	11	11–13	12	6.7–18	***3.5***	**2.2**	0.08	0
As	4.5	4.1–5.1	4.6	4.5–6.0	7.5	5.9–8.7	7.4	5.6–9.7	**0.6**	0.6	0.7	0
Cd	0.19	0.18–0.23	0.32	0.27–0.33	0.41	0.36–0.46	0.92	0.53–1.4	**0.5**	0.3	0.07	0
Ce	19	18–22	19	17–20	20	16–26	18	15–23	1.0	1.0	1	0
Co	18	18–19	15	12–17	12	12–16	8.5	7.4–13	**1.5**	1.8	0.2	0
Cr	130	92–140	89	87–95	190	170–230	130	84–140	**0.7**	0.7	10	0
Cs	0.98	0.87–1.0	0.93	0.79–1.0	0.56	0.55–0.66	0.93	0.78–1.0	1.8	1.0	0.01	0
Cu (mg/g)	0.57	0.36–0.67	0.35	0.27–0.46	1.2	1.2–2.0	0.83	0.82–0.98	***0.5***	**0.4**	0.008	0
Fe (mg/g)	40	37–42	33	26–34	47	33–49	32	16–35	0.8	1.0	0.1	0
Mn (mg/g)	0.59	0.58–0.62	0.47	0.41–0.56	0.52	0.49–0.58	0.55	0.38–0.57	1.1	0.8	0.001	0
Ni	41	35–53	40	34–44	30	28–48	33	31–51	1.3	1.2	5	0
Pb	19	11–35	22	21–30	48	31–69	29	29–30	0.4	0.7	10	0
Pt	< 0.4	< 0.4	< 0.4	< 0.4–0.09	< 0.4	< 0.4	< 0.4	< 0.4	–	–	0.4	85
Rb	23	23–26	24	22–26	15	13–16	18	12–20	1.6	1.4	0.3	0
Sb	88	47–100	43	32–59	150	120–240	90	52–93	**0.6**	0.5	0.1	0
Sc	11	10–12	7.1	6.6–11	3.1	3.0–3.9	1.9	1.7–4.9	***3.6***	**3.8**	0.05	0
Sn	100	76–110	96	52–120	190	180–280	100	39–100	**0.5**	1.0	20	0
Sr	96	92–130	120	81–150	200	130–210	150	140–390	0.5	0.8	50	5
Th	2.6	2.4–2.6	2.2	2.2–2.4	1.3	1.2–1.4	0.87	0.67–1.5	1.9	**2.5**	0.02	0
Tl	0.18	0.15–0.19	0.16	0.15–0.16	0.10	0.10–0.13	0.10	0.09–0.17	1.8	1.6	0.007	0
V	110	98–110	72	67–98	46	39–51	28	21–60	***2.4***	2.6	0.3	0
W	38	33–42	27	23–34	14	13–17	11	7.1–19	***2.8***	***2.4***	0.1	0
Zn (mg/g)	0.37	0.26–0.47	0.46	0.29–0.46	0.76	0.54–0.81	0.57	0.44–0.72	**0.5**	0.8	0.06	0

[a] Interquartile range
[b] Limit of detection.

(Supplementary Material; Tables 1–3). Fe, Al, and Ti were the major constituent elements of the PM, with concentrations in the ng/m^3 up to μg/m^3 range, followed by Zn, Cu, Mn, Ba, and Sr. Airborne element constituent levels were generally higher at Elgeseter compared to Torget station, but only a few of these differences were statistically significant. Levels of specific elements in PM were on average considerably higher in spring than in winter samples; this was especially the case for W, Ti, Sc, Al, V, Y, and Th in the $PM_{2.5–10}$ and $PM_{0.1}$ fractions. On the other hand, PM concentrations of some other elements, notably Pt, Cd, Bi, Cu, and Ba were on average highest in winter samples in all three size fractions. Other studies investigating elemental components of PM generally reported higher levels than in this study [27,28,30]. In addition to the presumed underestimation of

Table 3
Total element contents (in μg/g, unless otherwise stated) in road traffic (Elgeseter) and city background (Torget) $PM_{0.1–2.5}$ samples, collected in spring and winter (N = 5 from each site and for each season). p-values in bold signify statistical significance at the 0.05 level, whereas p-values in bold and italic signify statistical significance at the 0.01 level.

	Spring				Winter				Spring/winter ratio			
	Elgeseter		Torget		Elgeseter		Torget		Elgeseter	Torget		
	Median	IQR[a]	Median	IQR	Median	IQR	Median	IQR			LOD[b]	% < LOD
Al (mg/g)	8.2	5.2–13	5.8	5.2–8.9	4.5	3.7–6.9	2.5	2.2–6.9	1.8	2.3	0.1	0
As	35	19–39	31	30–37	68	59–75	66	59–84	**0.5**	0.5	1	0
Cd	3.7	3.0–5.0	4.7	4.0–5.4	7.1	6.1–7.4	7.8	7.7–8.8	**0.5**	0.6	0.1	0
Ce	14	14–15	15	11–15	11	9.1–12	16	8.3–33	1.3	0.9	2	0
Co	8.1	7.4–9.4	6.2	5.8–6.3	4.7	4.4–7.3	3.9	3.6–4.1	1.7	1.6	0.4	0
Cr	85	68–110	60	33–390	94	80–130	110	65–120	0.9	0.5	20	0
Cs	0.90	0.74–1.1	0.84	0.56–0.88	0.65	0.62–0.90	0.83	0.82–1.0	1.4	1.0	0.02	0
Cu (mg/g)	0.54	0.51–0.70	0.24	0.23–0.25	0.89	0.48–1.3	0.45	0.26–0.66	0.6	0.5	0.01	0
Fe (mg/g)	18	16–22	9.5	9.2–10	14	8.5–25	9.0	4.5–13	1.3	1.1	0.2	0
Mn (mg/g)	0.23	0.23–0.28	0.16	0.16–0.21	0.23	0.20–0.30	0.18	0.18–0.23	1.0	0.9	0.002	0
Ni	50	38–130	110	29–280	38	32–45	19	18–41	1.3	5.8	9	0
Pb	160	150–210	110	74–190	150	140–200	130	110–130	1.1	0.8	20	0
Pt	< 0.7	< 0.7	< 0.7	< 0.7	< 0.7	< 0.7	< 0.7	< 0.7	–	–	0.7	85
Rb	18	14–21	17	14–26	32	17–35	32	32–34	0.6	0.5	0.6	0
Sb	91	81–96	35	31–38	73	48–120	36	26–57	1.2	1.0	0.2	0
Sc	2.8	2.4–3.2	1.6	1.6–1.9	1.1	0.47–1.1	0.55	0.48–0.85	**2.7**	3.0	0.08	0
Sn	170	160–200	83	59–190	89	51–160	< 40	< 40	1.9	–	40	20
Sr	200	140–230	190	160–270	< 80	< 80–150	< 80	< 80–110	–	–	80	30
Th	0.93	0.71–1.4	0.72	0.65–1.2	0.43	0.39–0.58	0.34	0.26–0.37	**2.2**	**2.1**	0.04	0
Tl	0.45	0.39–0.61	0.44	0.40–0.57	0.49	0.39–0.50	0.67	0.62–0.74	0.9	0.7	0.01	0
V	35	34–44	37	36–42	24	16–25	18	18–23	***1.5***	***2.0***	0.5	0
W	13	12–14	5.7	5.6–6.9	5.9	2.2–11	3.6	1.4–4.3	**2.3**	1.6	0.2	0
Zn (mg/g)	1.3	0.91–1.5	0.95	0.71–1.3	1.2	1.1–1.2	1.0	0.95–1.2	1.1	1.0	0.1	0

[a] Interquartile range.
[b] Limit of detection.

Table 4
Total element contents (in μg/g, unless otherwise stated) in road traffic (Elgeseter) and city background (Torget) $PM_{0.1}$ samples, collected in spring and winter (N = 5 from each site and for each season). p-Values in bold signify statistical significance at the 0.05 level, whereas p-values in bold and italic signify statistical significance at the 0.01 level.

	Spring				Winter				Spring/winter ratio			
	Elgeseter		Torget		Elgeseter		Torget		Elgeseter	Torget		
	Median	IQR[a]	Median	IQR	Median	IQR	Median	IQR			LOD[b]	% < LOD
Al (mg/g)	19	16–27	15	13–21	3.2	2.9–6.3	7.3	6.6–11	***5.8***	**2.1**	0.2	0
As	11	8.4–16	19	17–27	28	26–54	58	50–71	**0.4**	**0.3**	2	0
Cd	1.4	1.3–1.7	3.1	2.1–3.2	6.4	2.8–8.1	8.3	8.2–8.8	**0.2**	***0.4***	0.2	0
Ce	18	7.4–21	18	10–18	11	6.6–13	14	12–18	1.6	1.3	3	0
Co	10	9.4–15	10	9.4–10	2.9	2.9–3.4	5.0	4.1–8.3	**3.3**	2.0	0.5	0
Cr	110	88–120	66	57–76	56	43–59	66	42–99	**2.0**	1.0	30	0
Cs	1.0	0.78–1.2	1.0	0.92–1.1	0.63	0.41–0.92	1.0	1.0–1.0	1.6	1.0	0.03	0
Cu (mg/g)	0.46	0.43–0.47	0.24	0.21–0.28	0.46	0.25–1.2	0.39	0.28–0.51	1.0	**0.6**	0.02	0
Fe (mg/g)	21	19–30	18	12–19	6.5	5.3–8.7	12	7.1–19	3.2	1.5	0.3	0
Mn (mg/g)	0.30	0.28–0.46	0.32	0.23–0.32	0.12	0.12–0.19	0.23	0.19–0.33	2.5	1.4	0.03	0
Ni	60	40–61	56	44–92	27	18–32	39	23–45	**2.2**	1.4	10	0
Pb	62	58–99	100	65–140	160	87–260	120	110–130	0.4	0.8	20	0
Pt	< 0.9	< 0.9	< 0.9	< 0.9	< 0.9	< 0.9	1.0	< 0.9–1.4	–	–	0.9	85
Rb	25	25–26	23	22–25	33	15–55	39	38–45	0.8	***0.6***	0.8	0
Sb	56	53–82	37	34–42	36	24–53	47	37–48	1.5	0.8	0.3	0
Sc	4.4	4.2–7.8	4.2	3.0–4.5	0.92	0.85–1.0	2.2	0.94–3.2	***4.7***	1.9	0.1	0
Sn	150	98–170	94	73–170	< 50	< 50–76	< 50	< 50	–	–	50	45
Sr	130	130–140	160	140–190	170	< 100–660	120	< 100–130	0.8	1.3	100	30
Th	1.8	1.7–2.1	1.1	1.1–2.1	0.27	0.24–0.47	0.65	0.45–0.87	***6.6***	***1.7***	0.1	0
Tl	0.27	0.27–0.36	0.37	0.34–0.39	0.63	0.40–0.65	0.68	0.65–0.73	**0.4**	***0.5***	0.02	0
V	49	49–85	58	56–61	14	11–16	34	20–37	**3.5**	***1.7***	1	0
W	17	15–22	11	10–12	2.8	1.3–3.7	5.3	2.5–6.3	**6.0**	**2.0**	0.2	0
Zn (mg/g)	0.74	0.63–1.0	0.75	0.56–0.77	1.3	0.39–1.6	1.2	1.2–1.2	0.6	0.6	0.1	0

[a] Interquartile range.
[b] Limit of detection.

total element contents discussed above, the sampling period was characterized by an exceptionally mild winter in addition to considerable precipitation, resulting in little re-suspension and quick deposition of dust. Cold periods with clear weather typically result in elevated levels of PM in urban areas [31,32]. The municipality also frequently swept the streets and applied $MgCl_2$ salt to reduce dust re-suspension, contributing further to the low PM levels observed in this study.

Element mass concentrations relative to total PM are shown in Tables 2-4 for $PM_{2.5–10}$, $PM_{0.1–2.5}$, and $PM_{0.1}$, respectively. The elements Al and Sc clearly accumulated in the coarse size fraction, as did Fe, Co, V, W, Th, and Mn in most samples (Table 2), indicating their origin mainly from re-suspension of crustal-derived soil dust by vehicles from the roads. Most of the studied elements accumulated in the fine fraction, indicating motor vehicular traffic as their main source (Table 3). Elemental constituent levels in the ultrafine fraction were quite low, and few elements accumulated in these particles (Cs, Pb, Pt, Rb, Sr, Tl, and Zn, Table 4), contrary to what might have been expected from their large numbers and surface area and thereby potential binding sites for elements. The similarity in elemental composition between the fine and the ultrafine size fraction indicates that the fine fraction may to a considerable degree consist of aggregated ultrafine primary particles. Size fraction distributions found in this study are mostly in agreement with other studies; crustal elements such as Al and Fe typically accumulate in the coarse fraction [33], whereas typical traffic-related elements such as Cu, Zn, Sb, Ni, Cr, and Mn are usually associated with the fine and partly ultrafine size fractions, several of these elements are reported to exhibit bimodal size distributions with peaks within the fine and nano size ranges [28]. Mn may also primarily originate from road dust re-suspension [34]. Gugamsetty et al. [27] found many elements including Cu, Zn, Sn, Ni, Cr, Co, Sr, and Pb to accumulate to a large extent in the ultrafine fraction. The finding that airborne concentrations of the majority of the elements were overall higher in the heavily trafficked Elgeseter area compared to the Torget city background station, supports the assumption that the main sources of elemental constituents of PM were vehicular emissions including exhaust and brake pad and tire wear, and vehicular re-suspension of road dust. Cd levels were higher at Torget station; the reason for this is not known.

3.4. Seasonal differences

Comparisons of elemental constituent concentrations between winter and spring seasons for the different size fractions revealed distinct seasonal patterns for many elements. Median Sc, W, and V concentrations in the dust were statistically significantly higher in spring than in winter samples in all three size fractions, pointing to higher contribution of crustal-derived soil particles. Al and Co were higher in spring samples in the coarse and ultrafine size fractions, and the same was true for Th in fine and ultrafine and Ni in ultrafine samples, all statistically significant. In areas with cold winters, resuspended road dust in spring typically contains smaller particles from road sand and salt applied during the winter season. Happo et al. [35] also found concentrations of the elements Al, Fe, and Mn to be overall highest in spring samples in $PM_{2.5–10}$ and $PM_{1–2.5}$ size fractions of air particulate samples collected in Helsinki, Finland.

3.5. Source analysis

Enrichment factors (EFs) are shown in Table 5. Elemental constituents in coarse particle ($PM_{2.5–10}$) samples with EFs >100 comprise, in order of decreasing EF: Sb > Sn; elements with EFs between 10 and 100 are: Cu > W > Zn > As > Pb (Table 5). Correspondingly, for the fine fraction ($PM_{0.1–2.5}$), elements with EFs above 100 are: Sb > Sn > As > Zn > Pb > Cu; elements with EFs between 10 and 100 are: W > Tl > Cr > Ni > Sr. For the ultrafine fraction ($PM_{0.1}$), elements with EFs above 100 are: Sb > Sn > As > Zn > Pb > Cu; elements with EFs between 10 and 100 are: W > Tl. These EF values, particularly those found in the fine and ultrafine fractions, are comparable to those found by Berg et al. [36], who studied trace elements in precipitation from selected rural and remote sites in Norway.

In the present study, EF values for Sb and Sn in the coarse fraction were found to be >100, so these elements almost certainly originate mainly from

Table 5
Enrichment factors (EFs) and Cu/Sb ratios in road traffic (Elgeseter) and city background (Torget) $PM_{2.5–10}$, $PM_{0.1–2.5}$, and $PM_{0.1}$ samples, collected in spring and winter (N = 5 from each site and for each season).

	$PM_{2.5–10}$								$PM_{0.1–2.5}$								$PM_{0.1}$					
	Spring				Winter				Spring				Winter				Spring				Winter	
	Elgeseter		Torget		Elgeseter		Torget		Elgeseter		Torget		Elgeseter		Torget		Elgeseter		Torget		Elgeseter		Torget	
	Mean	SD[a]	Mean	SD	Mean	SD	Mean	SD	Mean	SD	Mean	SD	Mean	SD	Mean	SD	Mean	SD	Mean	SD	Mean	SD	Mean	SD
Al	1		1		1		1		1		1		1		1		1		1		1		1	
As	5.8	1.0	8.6	1.7	27	11	36	21	200	160	220	82	1300	1700	1300	1000	32	10	73	58	720	740	600	670
Ce	0.73	0.058	0.90	0.14	2.2	1.1	2.1	1.0	3.1	2.3	3.5	1.5	5.5	5.2	7.8	2.6	1.0	0.24	1.2	0.54	5.2	5.0	4.4	4.5
Co	1.6	0.14	1.7	0.14	3.4	1.1	2.8	0.89	3.5	1.3	3.7	1.3	6.2	5.5	4.5	1.9	1.9	0.24	2.0	0.31	3.9	2.3	3.8	3.0
Cr	2.7	0.63	2.7	0.28	15	8.1	7.8	4.5	10	7.3	19	21	29	25	36	36	5.6	4.0	3.1	0.74	16	13	13	9.9
Cs	0.74	0.090	0.91	0.15	1.4	0.23	1.9	0.85	3.1	1.4	3.2	0.61	8.7	10	10	7.0	1.6	0.94	1.7	0.61	5.8	4.7	6.1	6.2
Cu	22	8.0	19	7.5	190	100	130	98	110	59	60	15	430	340	250	100	37	9.6	22	3.4	250	190	130	110
Fe	1.8	0.23	1.7	0.19	5.9	2.7	4.0	2.3	3.7	1.1	2.6	0.61	9.6	8.3	5.5	2.9	2.1	0.26	1.6	0.22	5.1	4.1	3.4	2.1
Mn	1.4	0.13	1.5	0.073	3.7	1.2	3.5	2.0	2.6	0.82	2.5	0.70	7.2	6.5	6.0	2.8	1.6	0.14	1.5	0.20	4.2	2.6	3.5	2.3
Ni	1.3	0.27	1.6	0.34	3.5	2.4	3.4	1.5	33	61	26	23	18	22	15	18	4.5	3.1	4.5	2.2	9.2	8.3	10	13
Pb	4.0	2.2	6.2	1.8	33	27	22	12	150	100	170	140	310	220	300	200	31	26	41	27	310	310	160	170
Rb	0.60	0.043	0.77	0.059	1.1	0.17	1.2	0.37	2.1	0.94	2.8	1.1	13	19	14	11	1.2	0.29	1.3	0.37	9.6	8.8	9.1	10
Sb	890	390	630	280	6200	3700	3400	3000	4800	2200	2400	790	13,000	12,000	6400	4000	1200	350	890	370	7000	6700	4100	4500
Sc	1.1	0.092	1.0	0.11	1.0	0.24	1.0	0.26	1.2	0.37	1.0	0.15	1.0	0.51	0.93	0.49	1.1	0.16	0.90	0.090	1.3	1.0	0.92	0.24
Sn	130	58	120	80	840	570	330	290	1100	890	980	780	1600	1300	460	210	340	210	410	420	920	940	410	530
Sr	0.68	0.11	1.0	0.44	3.4	2.2	5.5	5.4	7.1	6.5	6.9	3.4	13	13	13	17	2.3	2.2	2.5	1.8	14	8.0	11	12
Th	0.78	0.067	0.84	0.10	1.3	0.13	0.94	0.12	1.4	0.19	1.4	0.21	1.3	0.55	1.2	0.44	1.3	0.63	1.0	0.13	1.2	0.46	1.0	0.39
Tl	0.77	0.13	1.0	0.19	1.5	0.43	1.7	0.84	11	7.3	13	3.2	40	52	47	38	3.1	2.3	4.1	2.0	31	29	28	34
V	1.7	0.11	1.7	0.11	2.1	0.53	1.9	0.52	2.9	1.0	3.5	0.80	3.6	2.3	3.7	1.9	2.0	0.30	2.1	0.49	2.8	1.2	2.5	1.0
W	57	8.5	50	10	67	26	56	23	96	34	57	19	110	72	64	36	51	9.0	39	10	62	46	43	25
Zn	12	4.2	20	9.8	76	42	59	39	220	150	180	87	580	690	510	390	67	66	65	48	430	450	360	460
Cu/Sb	6.8		8.3		8.6		11		6.6		7.2		14		21		9.5		7.3		13		11	

[a] Standard deviation.

anthropogenic emission, most likely from motor vehicles. EF values for Sb were particularly high; Sb is known to be associated with brake pad wear in vehicles [37]. This finding is consistent with Asheim et al. [38], who found Sb to be a valuable marker for vehicular brake pad wear in road dust collected in Trondheim, Norway. Elements with EFs in the range 10–100 also most probably originate mainly from anthropogenic sources.

Element EF values were overall highest in fine, intermediate in ultrafine, and lowest in the coarse fraction. EF values for Elgeseter and Torget samples were comparable, with no statistical differences. For all three size fractions, EF values were considerably higher in winter than in spring samples. Sb clearly exhibited the highest EFs within all three size fractions, with average values of 6200, 13,000, and 7000 in Elgeseter winter samples in coarse, fine and ultrafine particles, respectively.

It must be kept in mind that EF values give only initial indications of anthropogenic origin, and have several limitations; for example, if the local soil has high levels of certain crustal elements, high EF values may be misinterpreted [39,40].

Elemental mass concentrations relative to total dust contents were subjected to PCA to further investigate and identify possible sources of the PM (Table 6). Bartlett's test was statistically significant for all three size fraction models, and the KMO measure gave values of 0.60, 0.84, and 0.52 for the coarse, fine and ultrafine PM models, respectively. Only two PCs were retained for all three size fraction PCA models since any additional PC contained high loadings due to elevated levels in only one or two individual samples. The $PM_{2.5–10}$, $PM_{0.1–2.5}$ and $PM_{0.1}$ PCA models explained 79%, 99% and 71% of the total variance in the data, respectively. The element variable loadings are illustrated graphically together with the sample scores for $PM_{2.5–10}$, $PM_{0.1–2.5}$, and $PM_{0.1}$ in the biplots shown in Fig. 2a–c, respectively.

For the $PM_{2.5–10}$ model, the elements Co, Mn, Rb, Cs, Tl, V, Ni, Ce, Th, Al, Sc, and Fe all load highly and W, Zn, and Cr intermediately onto the first PC (Table 7). Most of these elements are usually associated with crustal sources, and their EF values were low. It is therefore likely that resuspension of soil particles constituted the main source of these elements in coarse particles. W, on the other hand, had high EFs, and was probably primarily emitted by studded tire wear [38,41]. PC2 shows high loadings for Cu, Sb, Cr, Sn, and Pb, and partly for Zn, As, and Fe, all of which have been associated with trafficked urban areas [34]. Specifically Fe [42], Cu and Sb [37], Zn, Sn, Cr, and Ni [34] have in previous studies been linked to the wear of brake pads in motor vehicles. Zn [43], Cu, Sb, Sn, and Cr [34] have been associated with tire wear, and Ni and Zn with motor exhaust emissions [34], and As especially with diesel exhaust emissions [44].

For the $PM_{0.1–2.5}$ model, most elements are strongly positively correlated, with high negative loadings onto PC1 for all elements studied (Table 6, Fig. 2b), indicating that most elements seem to derive from traffic-related sources, probably vehicular resuspension of road dust consisting of mixtures of vehicular emission and soil components.

For the $PM_{0.1}$ model, typical crustal elements such as Sc, V, Co, Al, W, Mn, Th, Fe, and Ni load highly onto PC1 pointing to resuspension of soil particles, except for W which more likely originated from studded tire wear (Table 6, Fig. 2c). Elements apparently associated with motor vehicle emissions, including As, Cu, Zn, Pb, and Sb load onto PC2. Some of the elements most frequently associated with the Earth's crust, such as Rb and Tl, also load onto PC2, and several elements load intermediately onto both PC1 and PC2, such as Sb and Cs. This demonstrates how many elemental components of PM may have multiple sources.

Generally, source apportionment of PM near roads is difficult due to the mixture of emissions from exhaust, brake, tire, and pavement wear, and resuspension of road dust which originates from these sources in addition to crustal-derived soil particles [45]. Thorpe and Harrison [46] concluded that the Cu/Sb ratio in PM near roads is the best available marker of the contribution of emissions from the vehicles themselves, specifically brake wear, since the Cu/Sb ratio in brake dust of about 5:1 is markedly different from the typical ratio in the Earth's crust of about 125:1. Cu/Sb ratios found in this study ranged from 4.7 to 70, with average ratios of 8.7, 12, and 10 in all $PM_{2.5–10}$, $PM_{0.1–2.5}$, and $PM_{0.1}$ samples, respectively. Ratios were overall somewhat higher in Torget than in Elgeseter samples, and higher in winter than in spring samples (Table 5). The high Cu/Sb ratios, in addition to high EF values for Sb, clearly indicate dominance of vehicle-derived particles in the collected PM samples.

In this study, the PCA was limited by the small sample size, which resulted in individual deviant samples affecting the results to some degree. However, concentrations of PM and different components are typically highly variable, which affects most studies investigating PM size fraction distribution and component contents. The majority of the studied elements seem to originate from more than one source, as indicated by their significant loadings onto more than one PC, which complicates source apportionment. This is consistent with previous studies on PM source apportionment [28,34,47]. However, the results are only indicative of possible sources without additional data on composition and rate of the individual existing emissions.

Table 6
PCA loadings and percent variance explained for elemental concentrations relative to total dust contents for $PM_{2.5–10}$, $PM_{0.1–2.5}$, and $PM_{0.1}$. Loadings larger than 0.4 are shown in bold, and communalities lower than 0.5 are shown in italics.

	$PM_{2.5–10}$			$PM_{0.1–2.5}$			$PM_{0.1}$		
	PC1	PC2		PC1	PC2		PC1	PC2	
	50%	29%	Com.	98%	1%	Com.	44%	27%	Com.
Al	**0.82**	**−0.55**	0.98	**−0.99**	0.00	0.99	**−0.96**	0.14	0.94
As	0.38	**0.59**	*0.49*	**−0.98**	0.08	0.96	0.18	**−0.79**	0.66
Ce	**0.85**	0.22	0.77	**−1.00**	−0.01	0.99	**−0.65**	**−0.48**	0.66
Co	**0.97**	−0.15	0.96	**−1.00**	0.03	1.00	**−0.96**	−0.08	0.93
Cr	**0.44**	**0.84**	0.90	**−0.99**	−0.03	0.98	−0.35	−0.31	*0.22*
Cs	**0.89**	−0.17	0.81	**−1.00**	0.01	0.99	**−0.50**	**−0.67**	0.70
Cu	−0.05	**0.95**	0.91	**−0.95**	−0.28	0.97	0.02	**−0.79**	0.63
Fe	**0.77**	**0.48**	0.83	**−0.99**	0.07	0.99	**−0.92**	−0.30	0.93
Mn	**0.94**	0.18	0.92	**−1.00**	0.02	1.00	**−0.94**	−0.23	0.94
Ni	**0.86**	0.18	0.77	**−0.99**	0.03	0.98	**−0.70**	0.08	*0.49*
Pb	0.39	**0.75**	0.72	**−1.00**	0.01	1.00	0.24	**−0.78**	0.66
Rb	**0.89**	−0.27	0.87	**−0.99**	−0.02	0.98	0.13	**−0.94**	0.91
Sb	0.09	**0.90**	0.82	**−0.99**	0.05	0.97	**−0.44**	**−0.71**	0.70
Sc	**0.80**	**−0.54**	0.94	**−0.99**	0.07	0.99	**−0.98**	0.09	0.97
Sn	0.30	**0.83**	0.77	**−1.00**	0.02	1.00	**−0.48**	0.03	*0.23*
Sr	0.20	0.30	*0.13*	**−0.94**	−0.32	0.99	0.21	**−0.62**	*0.43*
Th	**0.83**	−0.40	0.84	**−0.98**	0.07	0.98	**−0.92**	0.22	0.89
Tl	**0.88**	−0.08	0.78	**−1.00**	0.04	0.99	**0.45**	**−0.70**	0.70
V	**0.86**	**−0.44**	0.94	**−1.00**	0.04	1.00	**−0.96**	0.06	0.93
W	**0.69**	**−0.46**	0.68	**−0.99**	0.07	0.99	**−0.95**	0.04	0.90
Zn	**0.67**	**0.61**	0.83	**−1.00**	0.01	0.99	0.16	**−0.79**	0.65

3.6. Element bioaccessibility

SLFs represent physiologically relevant extraction media to use as surrogates for the actual biological fluids [48]. Still it must be kept in mind that GMB and ALF are not identical in composition to lung cell interstitial and phagocyte fluid, respectively; proteins are replaced by organic acids for stability of the solutions [49]. Solubility of elements in SLFs may not correspond to the actual bioaccessibility and bioavailability of the elements in an individual person, as this would be highly variable depending on a number of factors such as wind speed and direction, precipitation and distance from the road, inhalation rate and mode, pathway, site and manner of deposition, and clearance rate and mode. *In vitro* and *in vivo* tests would give data on this variability, but such experiments are costly and pose ethical problems.

Element solubilities for the coarse, fine, and ultrafine fractions after extraction in GMB or ALF are presented in Tables 7–9. The results clearly show that the solubility for all elements is much higher for ALF than GMB extraction in all three size fractions. *E.g.* in the coarse fraction, mean As solubility after GMB extraction was 12% and 30% in Elgeseter and Torget samples, respectively, and correspondingly 58% and 75% after ALF extraction (Table 7). This is as expected as the pH of ALF is lower compared to the neutral GMB, and the results are in accordance with results from previous

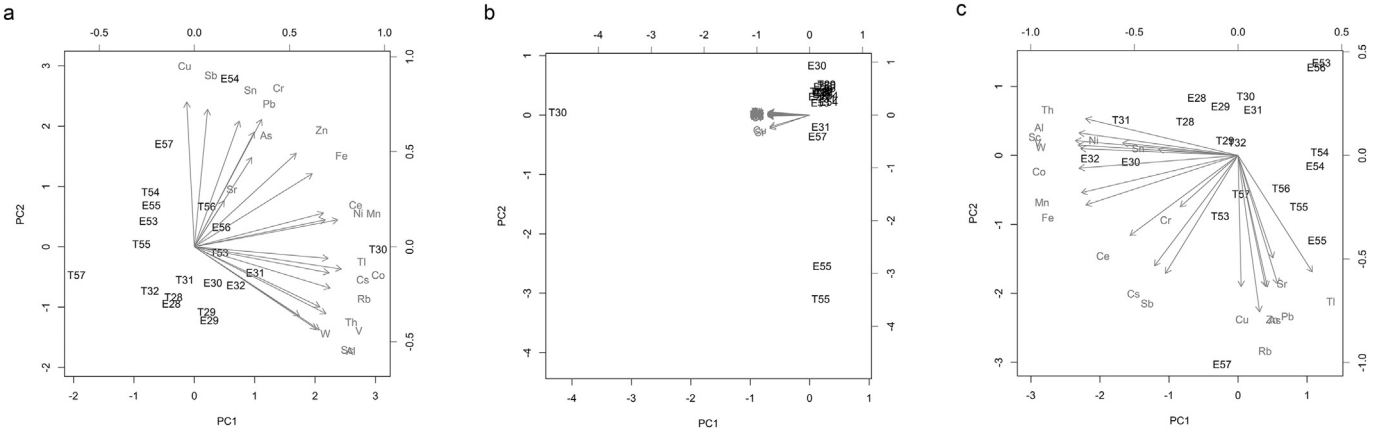

Fig. 2. PCA correlation biplots (2 PCs), showing elemental variable loadings and observation scores for a) $PM_{2.5–10}$, b) $PM_{0.1–2.5}$, and c) $PM_{0.1}$. Samples denoted E and T were collected at Elgeseter and Torget stations, respectively; sample numbers 28–32 were collected in spring and 53–57 were collected in winter.

studies comparing element solubility of PM in GMB and ALF [15–17]. Thus, solubility of some elemental constituents of PM in biological fluids within the lung may be substantial, especially if the particles are engulfed by phagocytes. Elements in dissolved form are more easily available for uptake by cells and subsequent exertion of toxic effects.

Overall, both GMB and ALF element solubility was higher in Torget than in Elgeseter samples; this is probably due to higher proportions of larger coarse particles with generally lower element solubility from resuspension of soil particles collected at the Elgeseter roadside as opposed to the city background station at Torget, which is higher above ground level. Overall GMB solubility in the different size fractions was as follows: $PM_{0.1–2.5} > PM_{0.1} > PM_{2.5–10}$. As an example average solubility of Tl was 15% and 42% in the coarse fraction of Elgeseter and Torget samples (Table 7), whereas corresponding values were 52% and 66% in fine (Table 8), and 36% and 55% in ultrafine PM (Table 9). Lower solubility of elemental components of ultrafine compared to fine particles appears surprising, as solubility might have been expected to increase with decreasing particle size since higher surface area would contain more potential binding sites for elements. However, Wiseman and Zereini [17] also reported high variability and no clear differences in element SLF solubility among PM_{10}, $PM_{2.5}$ and PM_1. A possible explanation for this finding is that the $PM_{0.1–2.5}$ size fraction may largely consist of aggregated ultrafine particles, resulting in little difference in elemental component bioaccessibility.

Individual element solubility values in simulated lung fluids were highly variable. In GMB, as an example, Tl solubility values in GMB for $PM_{2.5–10}$ ranged from 10% to 57% in Elgeseter and from 35% to 68% in Torget samples, and correspondingly from 5% to 64% in Elgeseter and from 45% to 74% in Torget samples in ALF (Table 7). Other studies have also shown such variability [16,17], and thus the identification of elements of special health concern with regard to solubility in SLFs is difficult. However, Rb, Tl, As, Zn, Ni, and W generally exhibited the highest solubilities in GMB, and correspondingly Cu, Sr, Pb, Zn, and Ni in ALF, whereas Fe, Al, and Sc exhibited overall low solubilities. Wiseman and Zereini [17] and Zereini et al. [16] obtained similar results; they found elevated solubilities for As and Sb in both solutions, whereas their V solubility in ALF was

Table 7
Element solubility (%) following extraction in Gamble's solution (GMB) and artificial lysosomal fluid (ALF) (%) for $PM_{2.5–10}$, with proportion of supernatant samples below LOD.

	GMB												ALF											
	Elgeseter						Torget						Elgeseter						Torget					
	n	Median	Mean	SD	Range	< LOD[a]	n	Median	Mean	SD	Range	< LOD[a]	n	Median	Mean	SD	Range	< LOD[a]	n	Median	Mean	SD	Range	< LOD[a]
Al	9	1.0	1.6	1.4	0.5–5.1	0.1	9	2.0	1.9	0.8	0.8–3.4	0.1	10	6.1	7.3	3.3	3.4–13	0	10	10	12	4.9	7.0–22	0
As	4	11	12	4.9	7.3–19	0.6	5	20	30	23	16–72	0.5	10	59	58	8.7	43–69	0	8	72	75	16	57–100	0.2
Ce	8	2.3	3.6	4.5	0.8–15	0.2	3	1.7	2.2	1.0	1.6–3.4	0.7	3	27	25	3.8	21–28	0.7	3	39	39	1.6	37–40	0.7
Co	10	11	10	3.0	5.1–13	0	9	12	12	4.2	6.6–18	0.1	10	35	37	6.7	27–48	0	10	46	48	8.8	35–64	0
Cr	0	–	–	–	–	1	0	–	–	–	–	1	8	20	21	4.6	12–28	0.2	3	37	38	4.6	35–43	0.7
Cs	3	5.0	6.6	3.8	4.0–11	0.7	2	32	32	34	8.0–57	0.8	4	29	29	5.4	22–35	0.6	3	30	36	12	27–50	0.7
Cu	8	11	10	3.6	5.1–15	0.2	6	19	19	3.3	16–24	0.4	10	82	78	12	51–89	0	10	90	90	1.9	86–93	0
Fe	8	0.8	2.1	3.3	0.2–10	0.2	7	1.3	1.3	0.3	0.9–1.7	0.3	10	24	29	13	12–49	0	10	39	38	14	20–59	0
Mn	10	4.1	5.8	3.5	2.2–11	0	9	5.9	6.5	2.0	4.2–9.9	0.1	10	31	37	12	20–54	0	10	47	52	18	30–81	0
Ni	1	14	14	–	–	0.9	1	20	20	–	–	0.9	2	31	31	6.5	26–35	0.8	1	66	66	–	–	0.9
Pb	2	8.3	8.3	6.7	3.6–13	0.8	0	–	–	–	–	1	5	83	83	11	73–100	0.5	6	86	84	4	75–87	0.4
Rb	0	–	–	–	–	1	1	67	67	–	–	0.9	7	17	23	13	14–50	0.3	9	38	43	21	20–76	0.1
Sb	10	7.4	8.1	4.9	2.8–17	0	10	13	14	6.0	5.2–25	0	10	74	70	17	26–85	0	10	80	80	4.2	74–87	0
Sc	2	1.2	1.2	0.9	0.5–1.8	0.8	1	16	16	–	–	0.9	9	5.0	7.5	4.3	3.7–15	0.1	8	8.5	10.0	5.5	5.2–22	0.2
Sn	4	2.5	2.5	1.0	1.3–3.7	0.6	1	2.1	2.1	–	–	0.9	10	50	52	16	21–73	0	10	92	84	21	38–100	0
Sr	0	–	–	–	–	1	0	–	–	–	–	1	3	46	49	17	33–67	0.7	1	69	69	–	–	0.9
Th	2	1.6	1.6	0.7	1.2–2.1	0.8	1	43	43	–	–	0.9	9	25	24	5.9	16–35	0.1	9	44	44	7	35–54	0.1
Tl	3	14	15	3.8	11–19	0.7	2	42	42	31	20–64	0.8	8	21	26	12	16–46	0.2	8	47	43	16	19–66	0.2
V	10	2.8	3.2	1.7	1.2–6.4	0	10	4.2	4.9	3.4	1.5–13	0	10	8.7	9.4	3.2	5.0–15	0	10	18	19	5.9	12–30	0
W	10	13	17	15	3.4–48	0	10	33	35	18	7.7–65	0	10	55	48	22	13–78	0	10	71	70	15	42–88	0
Zn	3	22	31	26	10–59	0.7	0	–	–	–	–	1	10	72	72	6.6	59–80	0	8	87	86	14	55–100	0.2

Table 8
Element solubility (%) following extraction in Gamble's solution (GMB) and artificial lysosomal fluid (ALF) (%) for $PM_{0.1–2.5}$, with proportion of supernatant samples below LOD.

	GMB												ALF											
	Elgeseter						Torget						Elgeseter						Torget					
	n	Median	Mean	SD	Range	< LOD	n	Median	Mean	SD	Range	< LOD	n	Median	Mean	SD	Range	< LOD	n	Median	Mean	SD	Range	< LOD
Al	7	3.8	3.5	1.4	1.6–5.4	0.3	7	4.9	7.5	4.9	3.5–16	0.3	10	14	16	9.5	5.9–34	0	10	15	18	11	9.4–47	0
As	10	42	43	11	30–59	0	10	68	69	5.3	60–79	0	10	79	76	16	43–100	0	10	77	75	8.7	57–87	0
Ce	3	3.9	3.8	2.4	1.4–6.2	0.7	3	0.8	1.3	0.9	0.7–2.3	0.7	0	–	–	–	–	1	1	29	29	–	–	0.9
Co	9	18	18	5.2	8.1–26	0.1	10	21	22	9.4	10–39	0	10	44	45	9.2	26–60	0	10	48	48	5.7	38–57	0
Cr	0	–	–	–	–	1	3	81	57	44	6.2–85	0.7	3	25	31	19	17–52	0.7	2	52	52	18	40–65	0.8
Cs	8	57	59	10	49–80	0.2	8	72	68	20	27–86	0.2	5	64	63	18	44–82	0.5	6	85	81	7.8	70–89	0.4
Cu	6	15	15	3.9	10–21	0.4	4	27	28	10	16–40	0.6	10	77	75	14	40–91	0	9	76	74	10	58–92	0.1
Fe	6	1.7	1.7	0.6	0.7–2.6	0.4	4	1.2	1.3	0.4	1.0–1.9	0.6	10	43	45	14	18–70	0	10	38	37	6.7	29–47	0
Mn	8	11	11	6.4	2.4–22	0.2	8	6.6	6.7	2.0	4.1–10	0.2	10	53	55	14	27–73	0	10	59	59	8.0	48–78	0
Ni	3	48	48	0.8	47–49	0.7	3	54	51	6.1	44–56	0.7	1	86	86	–	–	0.9	3	69	70	3.4	68–74	0.7
Pb	3	4.7	4.4	1.7	2.5–5.8	0.7	2	5.4	5.4	2.2	3.8–6.9	0.8	10	83	83	19	36–100	0	10	89	86	8.0	70–92	0
Rb	3	82	82	7.4	75–90	0.7	6	89	86	7.5	73–92	0.4	10	72	69	14	52–89	0	10	83	80	13	57–94	0
Sb	10	18	22	12	6.7–39	0	10	40	42	12	28–71	0	10	59	59	16	24–86	0	10	72	68	9.2	51–77	0
Sc	0	–	–	–	–	1	0	–	–	–	–	1	5	12	13	7.2	5.7–25	0.5	5	22	24	16	6.4–48	0.5
Sn	4	3.0	3.1	1.5	1.4–4.8	0.6	0	–	–	–	–	1	10	38	42	25	13–100	0	10	49	64	26	41–100	0
Sr	1	35	35	–	–	0.9	1	31	31	–	–	0.9	1	90	90	–	–	0.9	1	96	96	–	–	0.9
Th	0	–	–	–	–	1	0	–	–	–	–	1	6	38	35	13	13–50	0.4	5	42	46	9.7	35–60	0.5
Tl	10	54	52	12	33–69	0	10	67	66	8.5	50–79	0	10	73	70	9.9	50–84	0	10	72	74	5.2	67–81	0
V	10	28	27	15	6.4–48	0	10	47	46	15	9.7–61	0	10	42	42	16	13–66	0	10	57	54	15	17–71	0
W	9	15	14	5.5	4.2–22	0.1	10	26	27	12	15–57	0	10	29	34	23	13–87	0	10	43	46	12	26–62	0
Zn	3	27	24	5.4	18–27	0.7	0	–	–	–	–	1	10	79	77	13	42–88	0	10	89	88	6.4	78–100	0

considerably higher. Overall, these authors found slightly higher GMB solubilities for most elements compared to the present study.

4. Conclusions

Levels of total dust and elemental components of coarse, fine, and ultrafine PM in Trondheim city were generally low both at the motor vehicle traffic-dominated Elgeseter station and Torget city background station during the entire spring and winter sampling periods. However, dust and element concentrations were highly variable, showing increased levels in certain periods. Most elements accumulated within the fine size fraction, and to a lesser extent in ultrafine particles, whereas Al, and Sc, and to some extent Fe, Co, V, W, Th, and Mn accumulated in coarse particles. Overall, Al, Fe, Zn, Cu, Mn, and Sr, in decreasing order, exhibited the highest mass concentrations. Concentrations of typical crustal-derived elements such as Sc, Al, W, V, and Th were considerably higher in spring than in winter samples, whereas concentrations of As and Cd were highest in winter.

Enrichment factor (EF) analysis indicated that the majority of the studied elemental constituents in the coarse particles probably originated from resuspension of soil-derived road dust, whereas elements emitted from anthropogenic sources, primarily traffic-derived, seemed to accumulate in the fine and to some degree in the ultrafine size fractions. In coarse particles, elements with enrichment factors >100, indicating anthropogenic origin, comprised, in order of decreasing EF: Sb > Sn. Correspondingly, the following elements had EFs above 100 in the fine fraction: Sb > Sn > As >

Table 9
Element solubility (%) following extraction in Gamble's solution (GMB) and artificial lysosomal fluid (ALF) (%) for $PM_{0.1}$, with proportion of supernatant samples below LOD.

	GMB												ALF											
	Elgeseter						Torget						Elgeseter						Torget					
	n	Median	Mean	SD	Range	< LOD	n	Median	Mean	SD	Range	< LOD	n	Median	Mean	SD	Range	< LOD	n	Median	Mean	SD	Range	< LOD
Al	5	1.5	2.4	2.2	1.2–6.4	0.5	6	2.8	3.3	1.5	2.3–6.3	0.4	10	7.6	8.8	4.8	3.5–18	0	10	11	14	9.7	6.0–38	0
As	9	42	44	15	21–72	0.1	10	66	65	11	45–82	0	9	62	59	19	18–80	0.1	10	72	72	8.0	61–84	0
Ce	4	5.7	28.3	48	1.9–100	0.6	3	4.0	4.0	1.6	2.4–5.6	0.7	1	34	34	–	–	0.9	0	–	–	–	–	1
Co	5	15	17	4.0	13–23	0.5	8	21	19	6.3	6.5–24	0.2	9	41	38	9.0	21–50	0.1	10	47	45	7.5	29–53	0
Cr	0	–	–	–	–	1	0	–	–	–	–	1	1	16	16	–	–	0.9	2	70	70	24	53–87	0.8
Cs	6	49	45	20	21–74	0.4	7	57	53	20	15–74	0.3	1	29	29	–	–	0.9	2	72	72	9.5	65–78	0.8
Cu	2	15	15	8.3	9.5–21	0.8	1	21	21	–	–	0.9	8	70	73	7.4	65–84	0.2	10	83	82	5.9	69–90	0
Fe	5	1.7	1.8	0.7	1.2–2.8	0.5	3	2.2	2.3	0.6	1.8–2.9	0.7	10	27	28	14	3.9–51	0	10	32	32	5.7	21–40	0
Mn	8	8.0	13.2	17	1.3–52	0.2	9	5.8	5.5	2.2	1.7–8.2	0.1	8	45	43	10.7	29–57	0.2	10	52	51	10	38–71	0
Ni	2	82	82	26	63–100	0.8	1	49	49	–	–	0.9	1	68	68	–	–	0.9	1	74	74		74–74	0.9
Pb	2	8.4	8.4	4.5	5.2–12	0.8	0	–	–	–	–	1	7	75	70	16	42–90	0.3	9	78	78	4.2	71–84	0.1
Rb	3	80	76	12	63–86	0.7	5	78	77	4.3	70–81	0.5	8	48	48	22	21–73	0.2	10	61	60	15	37–82	0
Sb	9	22	25	17	9.1–62	0.1	10	30	31	10	15–52	0	10	58	50	20	12–75	0	10	69	69	5.5	57–76	0
Sc	1	18	18	–	–	0.9	0	–	–	–	–	1	6	9.1	23.8	37	4.8–98	0.4	5	11	11	2.5	8.3–15	0.5
Sn	2	100	100	–	–	0.8	0	–	–	–	–	1	8	33	38	14	24–66	0.2	10	100	94	17	45–100	0
Sr	1	100	100	–	–	0.9	0	–	–	–	–	1	1	72	72	–	–	0.9	1	72	72		72–72	0.9
Th	0	–	–	–	–	1	0	–	–	–	–	1	5	29	29	5.2	21–35	0.5	8	45	46	9.1	35–66	0.2
Tl	7	42	36	16	10–57	0.3	10	57	55	10	35–68	0	9	47	44	17	5.1–64	0.1	10	65	63	8.5	45–74	0
V	9	16	22	16	6.1–52	0.1	10	22	25	13	8.3–43	0	9	17	21	11	5.9–41	0.1	10	35	34	14	12–59	0
W	7	13	20	22	4.9–67	0.3	9	15	15	8.4	6.7–36	0.1	7	22	24	15	13–56	0.3	8	30	31	9.3	19–42	0.2
Zn	2	32	32	3.7	30–35	0.8	0	–	–	–	–	1	8	70	71	6.0	62–81	0.2	10	77	76	14	42–93	0

Table 10
Element solubility following extraction in Gamble's solution (GMB) and artificial lysosomal fluid (ALF) in the standard reference material Urban Particulate Matter 1648a (NIST), in % of certified values.

	GMB (N = 18)		ALF (N = 15)	
	Mean	SD	Mean	SD
Al	0.6	0.5	6.1	4.4
As	19	13	43	29
Ce	0.1	0.4	17	12
Co	9.9	5.6	16	11
Cr	0.5	0.5	4.8	4.8
Cu	5.7	4.4	21	21
Fe	0.3	0.2	8.3	6.3
Mn	6.3	3.3	31	16
Ni	9.4	6.0	15	10
Pb	0.6	0.8	26	29
Rb	9.9	4.2	11	5.4
Sb	9.2	5.6	22	16
V	8.4	7.0	22	20
Zn	0.8	0.6	23	20

Zn > Pb > Cu, and in the ultrafine fraction: Sb > Sn > As > Zn > Pb > Cu. EF values for Sb were especially high for all three size fractions, pointing to Sb as a suitable marker for road traffic emissions.

PCA applied to elemental relative to total dust mass concentrations identified vehicular resuspension of soil particles and emissions directly from motor vehicles as the two main probable sources of elemental constituents of all size fractions. Cu/Sb ratios in the PM samples indicate a predominance of vehicle-derived particles.

The solubility of elemental constituents was considerably higher in the more acidic ALF compared to the neutral GMB solution. Both GMB and ALF solubility was overall higher in Torget compared to Elgeseter samples. Surprisingly SLF solubility, although highly variable, was higher within the fine than the ultrafine fraction. Among the studied elements Rb, Tl, As, Zn, Ni, and W generally showed the highest solubility in GMB, whereas Cu, Sr, Pb, Zn, and Ni were the most soluble after ALF extraction.

Declaration of competing interest

The authors declare that they have no known competing financial or personal relationships that could have appeared to influence the work reported in this paper.

Acknowledgements

The project was partially funded by the Norwegian foundation “Anders Jahres fond til vitenskapens fremme”. We thank the Norwegian Public Roads Administration and Trondheim Municipality for permission to use their air measurement stations, and for assistance in installing the equipment. We thank Zahra Galal Mahmud for valuable assistance in collecting the samples and laboratory work. We also thank Prof. Bjørn Kåre Alsberg, Department of Chemistry, NTNU, for help and guidance with the multivariate data analysis techniques.

Appendix A. Supplementary data

Supplementary data to this article can be found online at https://doi.org/10.1016/j.enceco.2019.10.001.

References

[1] P.J. Landrigan, R. Fuller, N.J.R. Acosta, O. Adeyi, R. Arnold, N. Basu, et al., The Lancet Commission on pollution and health, Lancet 391 (2018) 462–512, https://doi.org/10.1016/S0140-6736(17)32345-0.
[2] E. Samoli, R. Peng, T. Ramsay, M. Pipikou, G. Touloumi, F. Dominici, et al., Acute effects of ambient particulate matter on mortality in Europe and North America: results from the APHENA study, Environ. Health Perspect. 116 (2008) 1480–1486, https://doi.org/10.1289/ehp.11345.
[3] B.R. Gurjar, A. Jain, A. Sharma, A. Agarwal, P. Gupta, A.S. Nagpure, et al., Human health risks in megacities due to air pollution, Atmos. Environ. 44 (2010) 4606–4613, https://doi.org/10.1016/j.atmosenv.2010.08.011.
[4] R. Beelen, M. Stafoggia, O. Raaschou-Nielsen, Z.J. Andersen, W.W. Xun, K. Katsouyanni, et al., Long-term exposure to air pollution and cardiovascular mortality, Epidemiology 25 (2014) 368–378, https://doi.org/10.1097/EDE.0000000000000076.
[5] World Health Organization (WHO) Europe, Air Quality Guidelines Global Update 2005 Particulate matter, ozone, nitrogen dioxide and sulfur dioxide. Germany, 2006.
[6] D.L. Costa, K.L. Dreher, Bioavailable transition metals in particulate matter mediate cardiopulmonary injury in healthy and compromised animal models, Environ. Health Perspect. 105 (Suppl. 5) (1997) 1053–1060.
[7] J.-C. Lee, Y.-O. Son, P. Pratheeshkumar, X. Shi, Oxidative stress and metal carcinogenesis, Free Radic. Biol. Med. 53 (2012) 742–757, https://doi.org/10.1016/j.freeradbiomed.2012.06.002.
[8] J.D. McNeilly, M.R. Heal, I.J. Beverland, A. Howe, M.D. Gibson, L.R. Hibbs, et al., Soluble transition metals cause the pro-inflammatory effects of welding fumes in vitro, Toxicol. Appl. Pharmacol. 196 (2004) 95–107, https://doi.org/10.1016/j.taap.2003.11.021.
[9] D. Wang, P. Pakbin, M.M. Shafer, D. Antkiewicz, J.J. Schauer, C. Sioutas, Macrophage reactive oxygen species activity of water-soluble and water-insoluble fractions of ambient coarse, PM2.5 and ultrafine particulate matter (PM) in Los Angeles, Atmos. Environ. 77 (2013) 301–310, https://doi.org/10.1016/j.atmosenv.2013.05.031.
[10] C.L.S. Wiseman, Analytical methods for assessing metal bioaccessibility in airborne particulate matter: a scoping review, Anal. Chim. Acta 877 (2015) 9–18, https://doi.org/10.1016/j.aca.2015.01.024.
[11] G. Herting, I. Odnevall Wallinder, C. Leygraf, Metal release from various grades of stainless steel exposed to synthetic body fluids, Corros. Sci. 49 (2007) 103–111, https://doi.org/10.1016/j.corsci.2006.05.008.
[12] O.R. Moss, Simulants of lung interstitial fluid, Health Phys. 36 (1979) 447–448.
[13] W. Stopford, J. Turner, D. Cappellini, T. Brock, Bioaccessibility testing of cobalt compounds, J. Environ. Monit. 5 (2003) 675–680.
[14] H. Scholze, R. Conradt, An in vitro study of the chemical durability of siliceous fibres, Ann Occup Hyg 31 (1987) 683–692, https://doi.org/10.1093/annhyg/31.4B.683.
[15] C. Colombo, A.J. Monhemius, J.A. Plant, Platinum, palladium and rhodium release from vehicle exhaust catalysts and road dust exposed to simulated lung fluids, Ecotoxicol. Environ. Saf. 71 (2008) 722–730, https://doi.org/10.1016/j.ecoenv.2007.11.011.
[16] F. Zereini, C.L.S. Wiseman, W. Püttmann, In vitro investigations of platinum, palladium, and rhodium mobility in urban airborne particulate matter (PM10, PM2.5, and PM1) using simulated lung fluids, Environ Sci Technol 46 (2012) 10326–10333, https://doi.org/10.1021/es3020887.
[17] C.L.S. Wiseman, F. Zereini, Characterizing metal(loid) solubility in airborne PM10, PM2.5 and PM1 in Frankfurt, Germany using simulated lung fluids, Atmos. Environ. 89 (2014) 282–289, https://doi.org/10.1016/J.ATMOSENV.2014.02.055.
[18] Statistics Norway, Befolkning og areal i tettsteder [In Norwegian], https://www.ssb.no/befolkning/statistikker/beftett/aar/2016-12-06 2017, Accessed date: 7 November 2017.
[19] Trondheim Municipality, The Norwegian Public Roads Authority, Pollution levels Trondheim, Norway, [In Norwegian] http://www.luftkvalitet.info/home.aspx?type=Area&id=%7Bba5403d7-522e-481b-a791-6148c8c6d0b4%7D 2018, Accessed date: 17 August 2018.
[20] European Commission (EC), Directive 2008/50/EC on ambient air quality and cleaner air for Europe 2008, http://eur-lex.europa.eu/LexUriServ/LexUriServ.do?uri=OJ:L:2008:152:0001:0044:en:PDF (accessed April 26, 2017).
[21] H. Weggeberg, T.F. Benden, E. Steinnes, T.P. Flaten, Element analysis and bioaccessibility assessment of ultrafine airborne particulate matter (PM0.1) using simulated lung fluid extraction (artificial lysosomal fluid and Gamble's solution), Environ Chem Ecotoxicol 1 (2019) 26–35, https://doi.org/10.1016/J.ENCECO.2019.08.001.
[22] European Committee for Standardization (CEN), EN 12341:2014 Ambient air - Standard gravimetric measurement method for the determination of the PM10 or PM2,5 mass concentration of suspended particulate matter, https://standards.cen.eu/dyn/www/f?p=204:110:0::::FSP_PROJECT,FSP_ORG_ID:29133,6245&cs=1DC6EB16DD302E384B46A7097AAC67CB5 2014, Accessed date: 7 November 2017.
[23] W.H. Zoller, E.S. Gladney, R.A. Duce, Atmospheric concentrations and sources of trace metals at the South Pole, Science 183 (1974) 198–200, https://doi.org/10.1126/science.183.4121.198(80-).
[24] B. Mason, C.B. Moore, Principles of geochemistry, 4th ed. John Wiley & Sons, 1982.
[25] R.C. Ragaini, H.R. Ralston, N. Roberts, Environmental trace metal contamination in Kellogg, Idaho, near a lead smelting complex, Environ. Sci. Technol. 11 (1977) 773–781, https://doi.org/10.1021/es60131a004.
[26] M.R. Flynn, Analysis of censored exposure data by constrained maximization of the Shapiro–Wilk W statistic, Ann. Occup. Hyg. 54 (2010) 263–271, https://doi.org/10.1093/annhyg/mep083.
[27] B. Gugamsetty, H. Wei, C.-N. Liu, A. Awasthi, S.-C. Hsu, C.-J. Tsai, et al., Source characterization and apportionment of PM 10 , PM 2.5 and PM 0.1 by using positive matrix factorization, Aerosol Air Qual. Res. 12 (2012) 476–491, https://doi.org/10.4209/aaqr.2012.04.0084.
[28] C.-C. Lin, S.-J. Chen, K.-L. Huang, W.-I. Hwang, G.-P. Chang-Chien, W.-Y. Lin, Characteristics of metals in nano/ultrafine/fine/coarse particles collected beside a heavily trafficked road, Environ. Sci. Technol. 39 (2005) 8113–8122.
[29] R. Beelen, O. Raaschou-Nielsen, M. Stafoggia, Z.J. Andersen, G. Weinmayr, B. Hoffmann, et al., Effects of long-term exposure to air pollution on natural-cause mortality: an analysis of 22 European cohorts within the multicentre ESCAPE project, Lancet 383 (2014) 785–795, https://doi.org/10.1016/S0140-6736(13)62158-3.
[30] S. Mbengue, L.Y. Alleman, P. Flament, Size-distributed metallic elements in submicronic and ultrafine atmospheric particles from urban and industrial areas in northern France, Atmos. Res. 135–136 (2014) 35–47, https://doi.org/10.1016/j.atmosres.2013.08.010.

[31] D.S. Lee, J.A. Garland, A.A. Fox, Atmospheric concentrations of trace elements in urban areas of the United Kingdom, Atmos. Environ. 28 (1994) 2691–2713, https://doi.org/10.1016/1352-2310(94)90442-1.
[32] D. Voutsa, C. Samara, T. Kouimtzis, K. Ochsenkühn, Elemental composition of airborne particulate matter in the multi-impacted urban area of Thessaloniki, Greece, Atmos. Environ. 36 (2002) 4453–4462, https://doi.org/10.1016/S1352-2310(02)00411-9.
[33] G.C. Lough, J.J. Schauer, J.-S. Park, M.M. Shafer, J.T. Deminter, J.P. Weinstein, Emissions of metals associated with motor vehicle roadways, Environ. Sci. Technol. 39 (2005) 826–836.
[34] F. Amato, M. Pandolfi, M. Viana, X. Querol, A. Alastuey, T. Moreno, Spatial and chemical patterns of PM 10 in road dust deposited in urban environment, Atmos. Environ. 43 (2009) 1650–1659, https://doi.org/10.1016/j.atmosenv.2008.12.009.
[35] M.S. Happo, M.-R. Hirvonen, A.I. Hälinen, P.I. Jalava, A.S. Pennanen, M. Sillanpää, et al., Seasonal variation in chemical composition of size-segregated urban air particles and the inflammatory activity in the mouse lung, Inhal. Toxicol. 22 (2010) 17–32, https://doi.org/10.3109/08958370902862426.
[36] T. Berg, O. Røyset, E. Steinnes, Trace elements in atmospheric precipitation at Norweigan background stations (1989–1990) measured by ICP-MS, Atmos. Environ. 28 (1994) 3519–3536, https://doi.org/10.1016/1352-2310(94)90009-4.
[37] J. Sternbeck, Å. Sjödin, K. Andréasson, Metal emissions from road traffic and the influence of resuspension—results from two tunnel studies, Atmos. Environ. 36 (2002) 4735–4744, https://doi.org/10.1016/S1352-2310(02)00561-7.
[38] J. Asheim, K. Vike-Jonas, S.V. Gonzalez, S. Lierhagen, V. Venkatraman, V. I-LS, et al., Benzotriazoles, benzothiazoles and trace elements in an urban road setting in Trondheim, Norway: Re-visiting the chemical markers of traffic pollution, Sci. Total Environ. 649 (2019) 703–711, https://doi.org/10.1016/J.SCITOTENV.2018.08.299.
[39] R.A. Duce, G.L. Hoffman, W.H. Zoller, Atmospheric trace metals at remote northern and southern hemisphere sites: pollution or natural? Science 187 (1975) 59–61, https://doi.org/10.1126/science.187.4171.59(80-).
[40] Reimann C, Caritat P de. Intrinsic flaws of element enrichment factors (EFs) in environmental geochemistry. Environ. Sci. Technol. 2000;34:5084–91. doi:https://doi.org/10.1021/es001339o.
[41] M. Bäckström, U. Nilsson, K. Håkansson, B. Allard, S. Karlsson, Speciation of heavy metals in road runoff and roadside total deposition, Water Air Soil Pollut. 147 (2003) 343–366, https://doi.org/10.1023/A:1024545916834.
[42] J.J. Schauer, G.C. Lough, M.M. Shafer, W.F. Christensen, M.F. Arndt, J.T. DeMinter, et al., Characterization of metals emitted from motor vehicles, Res. Rep. Health Eff. Inst. (2006) 1–76[discussion 77–88].
[43] K. Adachi, Y. Tainosho, Characterization of heavy metal particles embedded in tire dust, Environ. Int. 30 (2004) 1009–1017, https://doi.org/10.1016/j.envint.2004.04.004.
[44] S.M. Talebi, M. Abedi, Determination of arsenic in air particulates and diesel exhaust particulates by spectrophotometry, J. Environ. Sci. (China) 17 (2005) 156–158.
[45] F. Amato, F.R. Cassee, H.A.C. Denier van der Gon, R. Gehrig, M. Gustafsson, W. Hafner, et al., Urban air quality: the challenge of traffic non-exhaust emissions, J. Hazard. Mater. 275 (2014) 31–36, https://doi.org/10.1016/j.jhazmat.2014.04.053.
[46] A. Thorpe, R.M. Harrison, Sources and properties of non-exhaust particulate matter from road traffic: a review, Sci. Total Environ. 400 (2008) 270–282, https://doi.org/10.1016/j.scitotenv.2008.06.007.
[47] G.M. Marcazzan, S. Vaccaro, G. Valli, R. Vecchi, Characterisation of PM10 and PM2.5 particulate matter in the ambient air of Milan (Italy), Atmos. Environ. 35 (2001) 4639–4650, https://doi.org/10.1016/S1352-2310(01)00124-8.
[48] A. Mukhtar, A. Limbeck, Recent developments in assessment of bio-accessible trace metal fractions in airborne particulate matter: a review, Anal. Chim. Acta 774 (2013) 11–25, https://doi.org/10.1016/j.aca.2013.02.008.
[49] M. Takaya, Y. Shinohara, F. Serita, M. Ono-Ogasawara, N. Otaki, T. Toya, et al., Dissolution of functional materials and rare earth oxides into pseudo alveolar fluid, Ind. Health 44 (2006) 639–644.